

# Detecting metrologically useful entanglement in the vicinity of Dicke states

Iagoba Apellaniz<sup>1</sup>, Bernd Lücke<sup>2</sup>, Jan Peise<sup>2</sup>, Carsten Klempt<sup>2</sup>, Géza Tóth<sup>1,3,4</sup>

<sup>1</sup> Department of Theoretical Physics, University of the Basque Country UPV/EHU, P.O. Box 644, E-48080 Bilbao, Spain

<sup>2</sup> Institut für Quantenoptik, Leibniz Universität Hannover, Welfengarten 1, 30167 Hannover, Germany

<sup>3</sup> IKERBASQUE, Basque Foundation for Science, E-48013 Bilbao, Spain

<sup>4</sup> Wigner Research Centre for Physics, Hungarian Academy of Sciences, P.O. Box 49, H-1525 Budapest, Hungary

E-mail: iagoba.apellaniz@gmail.com, toth@alumni.nd.edu

PACS numbers: 03.67.Mn, 03.75.Gg, 03.75.Dg, 42.50.St

**Abstract.** We present a method to verify the metrological usefulness of noisy Dicke states of a particle ensemble with only a few collective measurements, without the need for a direct measurement of the sensitivity. Our method determines the usefulness of the state for the usual protocol for estimating the angle of rotation with Dicke states, which is based on the measurement of the second moment of a total spin component. It can also be used to detect entangled states that are useful for quantum metrology. We test our approach on recent experimental results.

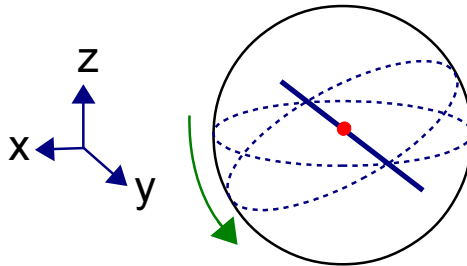


**Figure 1.** Metrology with symmetric Dicke states on the multiparticle Bloch sphere. In a linear interferometer, the uncertainty ellipse of the state is rotated around the  $y$  axis, while the rotation angle is estimated by collective measurements.

## 1. Introduction

Quantum metrology is concerned with metrological tasks in which the quantumness of the system plays an essential role [1, 2, 3, 4, 5]. One of its key goals is identifying bounds for the highest precision achievable in parameter estimation tasks in a quantum system, for example, by using the theory of quantum Fisher information [6, 7, 8, 9, 10]. Recently, there has been a large effort connecting quantum metrology to quantum information science, in particular, to the theory of quantum entanglement [11]. It has turned out that, in linear interferometers, entanglement is needed to surpass the shot-noise limit corresponding to product states [12]. It has been shown that fully entangled multipartite quantum states are needed to reach the maximal precision [13, 14, 15]. In particular, the quantum Fisher information, a fundamental quantity in metrology, can be used to detect multipartite entanglement.

After the theoretical findings mentioned above, it is crucial to know how large precision can be achieved in realistic, noisy systems [16, 17]. Thus, quantum metrology has been a driving force behind the numerous recent quantum optics experiments with cold gases and cold trapped ions, which were possible due to the rapid technological advancement in the field [18, 19, 20, 21]. Quantum metrology played a central role even in the recent experiments with the squeezed-light-enhanced gravitational wave detector GEO 600 [22].

There have been many experiments with fully polarized atomic ensembles in which the collective spin of the particles is rotated around an axis perpendicular to the mean spin (for instance by a homogeneous magnetic field) and the angle of the rotation is estimated based on collective measurements. It has also been verified experimentally that spin squeezing can result in a better precision compared to fully polarized product states (i.e.,  $SU(2)$  coherent states) [23, 24, 25, 26, 27, 28, 29, 30, 20, 31, 32] since spin-squeezed states are characterized by a reduced uncertainty in a direction orthogonal to the mean spin [33, 34, 35, 36]. A method has been presented for detecting metrologically useful entanglement for spin-squeezed states based on collective measurements [12].

Besides almost fully polarized states, there are also unpolarized states considered

for quantum metrology. Prime examples of such states are Greenberger-Horne-Zelinger (GHZ) states [37], which have already been realized experimentally many times [38, 39, 40, 41, 42, 18, 43, 44]. Recently, new types of unpolarized states have been considered for metrology, such as singlet states [45, 46] and symmetric Dicke states realized in cold gases and photons [47, 48, 49, 50]. In the metrological schemes with Dicke states, the state is rotated around an axis in a linear interferometer and the rotation angle is estimated based on collective measurements (see figure 1). For this case, a criterion to detect the metrological usefulness of some of these states has been derived for symmetric systems [51]. There is another criterion based on an improved Heisenberg relation to bound the quantum Fisher information close to Dicke states [52]. However, these criteria show metrological usefulness allowing for arbitrary measurements using the theory of the quantum Fisher information, while it might be interesting to show metrological usefulness for the measurements carried out in a particular metrological scheme. For example, in a large ensemble, we can allow for collective measurements only.

In this paper, we present a condition for metrological usefulness for the case when the second moment of a spin component of the state is measured to obtain an estimate for the rotation angle. Our findings are expected to simplify the experimental determination of metrological sensitivity since the proposed set of a few collective measurements is much easier to carry out than determining the metrological sensitivity directly. Our method is optimal in the sense that it gives the precision of the parameter estimation exactly, if certain operator expectation values are provided. If not all relevant expectation values can be measured, it can still give useful bounds. We also test our approach using data of a recent experiment realizing parameter estimation with a Dicke state [53]. Thus, our paper is expected to be useful for similar experiments in the future. Since quantum states with a metrological sensitivity larger than a certain bound are entangled [12], our method can also be used to detect metrologically useful entanglement in the vicinity of Dicke states. Note, however, that our work is not related to the criterion presented in [53], which detects multipartite entanglement in particle ensembles independently from metrological applications.

Our paper is organized as follows. In section 2, we discuss the basics of quantum metrology. In section 3, we present our criterion. In section 4, we compare our criterion to the sensitivity bound obtained from the quantum Fisher information. In section 5, we show how to apply our criterion to experimental results.

## 2. Basics of quantum metrology

In this section, we review the basics of quantum metrology. We discuss how the precision of the parameter estimation can be calculated, and how it can be bounded by the quantum Fisher information. We also discuss how the precision is linked to the entanglement of the quantum state.

One of the most fundamental tasks in quantum metrology is the estimation of the

small phase  $\theta$  in the unitary dynamics

$$\varrho_\theta = e^{-iH\theta} \varrho e^{+iH\theta}, \quad (1)$$

where  $H$  is the Hamiltonian of the dynamics,  $\varrho$  is the initial state, and  $\varrho_\theta$  is the final state after the evolution. The parameter  $\theta$  must be estimated based on measuring an observable  $M$  on the final state.

Next, we will discuss how to estimate the uncertainty of the parameter estimation. The variance of the estimated parameter can be calculated by the error propagation formula as

$$(\Delta\theta)^2 = \frac{(\Delta M)^2}{|\partial_\theta \langle M \rangle|^2}. \quad (2)$$

One can interpret (2) as follows. The larger the variance of  $M$ , the worse the precision. On the other hand, the larger the derivative of the expectation value of  $M$ , the better the precision.

Some operators are better than others for parameter estimation with a certain quantum state. The quantum Cramér-Rao inequality gives a lower bound on (2) that cannot be surpassed by any choice of  $M$ . In this paper, we will use many times the Cramér-Rao inequality formulated with the reciprocal of  $(\Delta\theta)^2$  as

$$(\Delta\theta)^{-2} \leq F_Q[\varrho, H], \quad (3)$$

where  $F_Q$  is the quantum Fisher information [6, 7, 8, 9]. It has been shown that the bound in (3) can be saturated by some measurement, and there is even a formula to find the optimal observable [8]. Note that all these are valid in the limit of infinite repetitions of the measurement, from which the expectation values can be obtained exactly. The case of finite number of measurements is more complicated [3, 4].

In certain situations, it is better to use (2) rather than (3) for calculating the best precision achievable, since it gives the precision for a particular operator to be measured in an experimental setup. This is reasonable since in a typical experiment, only a restricted set of operators can be measured. In this article, we will consider many-particle systems in which the particles cannot be addressed individually, and only collective quantities can be measured. In particular, in such a multiparticle system, we can measure the collective angular momentum operators

$$J_l = \sum_{n=1}^N j_l^{(n)}, \quad (4)$$

for  $l = x, y, z$ , and  $j_l = \frac{1}{2}\sigma_l$ , where  $\sigma_l$  are the Pauli spin matrices. Moreover,  $N$  is the number of pseudo-spin- $\frac{1}{2}$  particles.

Using collective angular momentum operators, it is even possible to connect the metrological precision to quantum entanglement [54, 55]. Let us briefly review some notions of entanglement theory. Separable states are mixtures of multiparticle products states. If a state is not separable then it is called entangled. Entangled states can be used as a resource for several quantum information processing tasks [55]. It has turned

out that certain entangled states are also useful for quantum metrology. In particular, if a quantum state fulfills

$$F_Q[\varrho, J_l] > N, \quad (5)$$

then it is entangled [12]. As a consequence of (2), (3) and (5), if

$$\frac{|\partial_\theta \langle M \rangle|^2}{(\Delta M)^2} > N \quad (6)$$

holds, then the system is also entangled. Hence, entanglement is required for a large metrological precision.

Finally, it is even possible to find bounds for states with various forms of multipartite entanglement. Let us review very briefly the definitions needed to characterize multipartite entanglement. A pure state containing at most  $k$ -particle entanglement is of the form

$$|\Psi_{k\text{-particle ent.}}\rangle = |\psi_1\rangle \otimes |\psi_2\rangle \otimes \dots \otimes |\psi_M\rangle, \quad (7)$$

where  $|\psi_k\rangle$  are quantum states of at most  $k$  qubits. A mixed state containing at most  $k$ -particle entanglement is a mixture of pure states of the form (7) [35, 56, 57]. Recently, it has been shown that if

$$F_Q[\varrho, J_l] > kN \quad (8)$$

holds for a quantum state, then it is at least  $(k+1)$ -particle entangled [13, 14] †. Another formulation is saying that the entanglement depth of the state is at least  $(k+1)$  [35]. Similarly to the previous paragraph, it follows that a quantum state is at least  $(k+1)$ -particle entangled if

$$\frac{|\partial_\theta \langle M \rangle|^2}{(\Delta M)^2} > kN \quad (9)$$

holds.

Based on this section, one can see the advantages of using the quantity  $(\Delta\theta)^{-2}$  rather than  $(\Delta\theta)^2$  in our discussion. It can be directly compared to the quantum Fisher information [see (3)]. Moreover,  $(\Delta\theta)^{-2}/N$  directly leads to a lower bound on the entanglement depth. Note the relation of  $(\Delta\theta)^{-2}$  to the precision: it is large for a high precision and small for a low precision.

### 3. Metrology with Dicke states

In this section, we will consider metrology with symmetric Dicke states [58]. In particular, we will consider symmetric states that are the eigenstates of  $J_z$  with a zero eigenvalue. The metrological setup is the following. The Dicke state is rotated around the  $y$  axis of the multiparticle Bloch sphere. Then, we estimate the rotation angle by

† Equation (8) is valid if  $k$  is a divisor of  $N$ . The general formula is somewhat more complicated than (8) [13, 14]. Equation (8) can also be used if  $k \ll N$ , since in this case the difference between (8) and the general formula is small. Note that  $k \ll N$  is fulfilled in practice in many experiments.

collective measurements. Such an experiment has already been carried out in cold gases [47]. It was found that for noisy states, the optimal angle for parameter estimation is not  $\theta = 0$ . Thus, (2) was recorded for many different values of  $\theta$ . The phase estimation uncertainty was then plotted as a function of the rotation angle  $\theta$ , and the best precision could be identified. In this section, we will show that the optimal angle can be obtained easily as a closed formula. We even find a closed formula for the maximal parameter estimation precision, as a function of a few expectation values. In this way, one can verify the metrological usefulness of the state without directly probing the phase estimation uncertainty for many phases.

Next, let us define the Dicke states, and examine their metrological properties. A  $N$ -qubit symmetric Dicke state is given as

$$|D_N^{(m)}\rangle = \binom{N}{m}^{-\frac{1}{2}} \sum_k \mathcal{P}_k(|1\rangle^{\otimes m} \otimes |0\rangle^{\otimes(N-m)}), \quad (10)$$

where the summation is over all the different permutations of the product state having  $m$  particles in the  $|1\rangle$  state and  $(N - m)$  particles in the  $|0\rangle$  state. One of such states is the  $W$ -state for which  $m = 1$ , which has been prepared with photons, ions, and neutral atoms [59, 60, 61].

From the point of view of metrology, we are interested mostly in the symmetric Dicke state for even  $N$  and  $m = \frac{N}{2}$ . This state is known to be highly entangled [62, 63] and allows for Heisenberg-limited interferometry [64]. In the following, we will omit the superscript giving the number of  $|1\rangle$ 's and use the notation

$$|D_N\rangle \equiv |D_N^{(\frac{N}{2})}\rangle. \quad (11)$$

Symmetric Dicke states of the type (11) have been created in photonic systems [65, 66, 50, 49, 67], in cold gases [47, 48, 53] and recently in trapped cold ions [68], and their metrological properties have also been verified experimentally [47, 49].

How can we do metrology with a  $|D_N\rangle$  state, taking into account even the practical case of a nonideal Dicke state? We will consider a general initial state  $\varrho$ , rather than the special case of a Dicke state. We will study a scheme in which the state is rotated around the  $y$  axis, corresponding to a unitary evolution under the Hamiltonian

$$H_D = J_y. \quad (12)$$

Then, we measure  $\langle J_z^2 \rangle$  to obtain an estimate for the angle of rotation. The error propagation formula (2) gives us the variance of the parameter estimation as

$$(\Delta\theta)^2 = \frac{(\Delta J_z^2)^2}{|\partial_\theta \langle J_z^2 \rangle|^2}. \quad (13)$$

Next, we calculate the quantities in (13) one after the other. For that, we need to use the dynamics of  $J_z$  given in the Heisenberg picture as

$$J_z(\theta) = e^{iJ_y\theta} J_z e^{-iJ_y\theta}. \quad (14)$$

In the following, all operators evolve according to the Heisenberg picture and all expectation values are calculated for the initial state  $\varrho$ .

Before continuing our calculations, we need to make an important simplifying assumption. We will assume that for all  $\theta$

$$\begin{aligned}\langle J_z^2(\theta) \rangle &= \langle J_z^2(-\theta) \rangle, \\ \langle J_z^4(\theta) \rangle &= \langle J_z^4(-\theta) \rangle\end{aligned}\tag{15}$$

holds. Equation (15) implies that the two expectation values must be even functions of  $\theta$ , and that we can omit the terms that are odd in  $\theta$ . In section 5, we will see that unitary dynamics starting from the experimentally prepared state have the property (15).

Let us now continue computing the precision given by (13). First, let us calculate the numerator of (13). Using (14) to obtain the dynamics, and with our simplifying assumptions (15) we arrive at

$$\begin{aligned}\langle J_z^2(\theta) \rangle &= \langle J_z^2 \rangle \cos^2 \theta + \langle J_x^2 \rangle \sin^2 \theta, \\ \langle J_z^4(\theta) \rangle &= \langle J_z^4 \rangle \cos^4 \theta + \langle J_x^4 \rangle \sin^4 \theta \\ &\quad + \left( \langle \{J_z, J_x\}^2 \rangle + \langle \{J_z^2, J_x^2\} \rangle \right) \cos^2 \theta \sin^2 \theta,\end{aligned}\tag{16}$$

where  $\{X, Y\} = XY + YX$  is the anticommutator of  $X$  and  $Y$ . Then, we calculate the denominator of (13). Using the dynamics of  $\langle J_z^2(\theta) \rangle$  given in (16) and the assumption in (15), we obtain the derivative as

$$\partial_\theta \langle J_z^2 \rangle = 2(\langle J_x^2 \rangle - \langle J_z^2 \rangle) \cos \theta \sin \theta.\tag{17}$$

The details of our calculations are given in appendix A.

Substituting (16) and (17) into the error propagation formula (13), after straightforward algebra, we arrive at a simple expression for the parameter variance

$$(\Delta\theta)^2 = \frac{(\Delta J_x^2)^2 f(\theta) + 4\langle J_x^2 \rangle - 3\langle J_y^2 \rangle - 2\langle J_z^2 \rangle(1 + \langle J_x^2 \rangle) + 6\langle J_z J_x^2 J_z \rangle}{4(\langle J_x^2 \rangle - \langle J_z^2 \rangle)^2},\tag{18}$$

where

$$f(\theta) := \left[ \frac{(\Delta J_z^2)^2}{(\Delta J_x^2)^2} \frac{1}{\tan^2 \theta} + \tan^2 \theta \right].\tag{19}$$

For the details of the calculation, see appendix B.

Next, we determine the optimal angle  $\theta$  that minimizes the parameter variance (18). It is easy to see that the optimal angle has to minimize also (19). The angle minimizing (19) is given by

$$\tan^2 \theta_{\text{opt}} = \sqrt{\frac{(\Delta J_z^2)^2}{(\Delta J_x^2)^2}}.\tag{20}$$

Equation (20) makes it possible to plan an experiment for the verification of the maximal accuracy such that we do not need to measure the sensitivity for a large range of  $\theta$ 's, but can target the parameter values close to the optimal angle.

Remarkably, we can even use (20) to obtain an explicit formula from (18) for the minimal parameter variance achievable by the setup as

$$(\Delta\theta)_{\text{opt}}^2 = \frac{2\sqrt{(\Delta J_z^2)^2(\Delta J_x^2)^2 + 4\langle J_x^2 \rangle - 3\langle J_y^2 \rangle - 2\langle J_z^2 \rangle(1 + \langle J_x^2 \rangle) + 6\langle J_z J_x^2 J_z \rangle}}{4(\langle J_x^2 \rangle - \langle J_z^2 \rangle)^2}.\tag{21}$$

For the evaluation of (21), we do not need to make a direct measurement of the sensitivity for some range of  $\theta$  in the vicinity of  $\theta_{\text{opt}}$ . We need to measure only the expectation values  $\langle J_x^2 \rangle$ ,  $\langle J_y^2 \rangle$ ,  $\langle J_z^2 \rangle$ ,  $\langle J_x^4 \rangle$ ,  $\langle J_z^4 \rangle$ , and  $\langle J_z J_x^2 J_z \rangle$  of the initial state (i.e., at  $\theta = 0$ ), which could make the experiments much easier. Later, we will discuss how to avoid measuring  $\langle J_z J_x^2 J_z \rangle$ , and even avoiding measuring the fourth order moments.

Finally, let us demonstrate the correctness of our formula (21) for the pure Dicke state  $|D_N\rangle$ . For this purpose, we will summarize the expectation values of the relevant moments of some collective observables for the state. Our Dicke state is an eigenstate of  $J_z$  with an eigenvalue zero. Hence, it immediately follows that

$$\langle J_z^2 \rangle = 0, \quad \langle J_z^4 \rangle = 0, \quad \langle J_z J_x^2 J_z \rangle = 0. \quad (22)$$

Moreover we know that for every quantum state

$$\langle J_x^2 \rangle + \langle J_y^2 \rangle + \langle J_z^2 \rangle \leq \frac{N(N+2)}{4} \quad (23)$$

holds, while symmetric quantum states, such as the Dicke state  $|D_N\rangle$ , saturate the inequality. Based on (22) and (23), and knowing that the rotational symmetry around the  $z$  axis implies  $\langle J_x^2 \rangle = \langle J_y^2 \rangle$ , we arrive at

$$\langle J_x^2 \rangle = \langle J_y^2 \rangle = \frac{N(N+2)}{8}. \quad (24)$$

Somewhat technical, but straightforward algebra leads to

$$\langle J_x^4 \rangle = \langle J_y^4 \rangle = \frac{(N+2)}{8} \left( \frac{3N(N+2)}{16} - \frac{1}{2} \right), \quad (25)$$

which will be useful later in the article. Equations (22) and (24) are sufficient to evaluate (21), and we obtain

$$(\Delta\theta)_{\text{opt}}^2 = \frac{2}{N(N+2)}, \quad (26)$$

which reproduces the value given by the quantum Fisher information [47]. Hence, for this case the Cramér-Rao bound (3) is saturated, which also means that  $J_z^2$  is the optimal operator to measure for the ideal Dicke state. In addition, (20) yields that the optimal angle for the ideal Dicke state (11) is  $\theta_{\text{opt}} = 0$ .

#### 4. Testing our bound on concrete examples

In this section, we compare our formula (21) for  $(\Delta\theta)_{\text{opt}}^2$  with the bound obtained from the quantum Fisher information. We find that the formula gives a good lower bound on the quantum Fisher information using the inequality  $(\Delta\theta)_{\text{opt}}^{-2} \leq F_Q[\varrho, J_y]$ . It has been mentioned in the introduction that our formula yields the best precision assuming that  $\langle J_z^2 \rangle$  is measured after the linear interferometer. If a different operator is measured, then the precision can even be higher. The quantum Fisher information gives us a bound on the precision if any measurement is allowed. However, note that in the latter case the optimal measurement might turn out to be impractical.



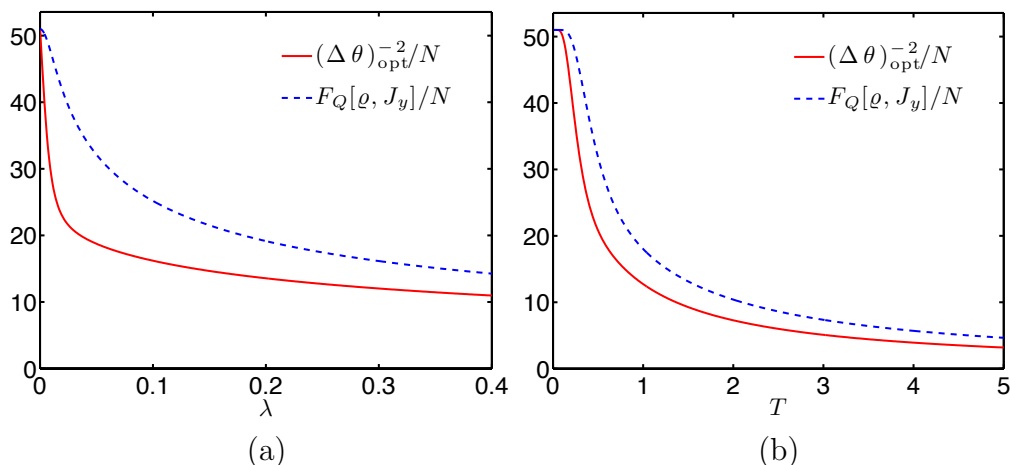


**Figure 2.** (a) The reciprocal of the parameter variance  $(\Delta\theta)_{\text{opt}}^2$  given in (21) and the quantum Fisher information for the ground states of the spin-squeezing Hamiltonian (27) as a function of  $\lambda$  for  $N = 100$  particles. (b) The same quantities are shown for the thermal states (29) as a function of  $T$ .

Let us consider first the example of pure spin-squeezed states obtained as a ground state of the spin squeezing Hamiltonian

$$H_{\text{sq}}(\lambda) = J_z^2 - \lambda J_x, \quad (27)$$

where  $\lambda$  is a real parameter. For  $\lambda > 0$ , the ground state is unique, and it is in the symmetric subspace. Hence, we can use the  $SU(2)$  generators instead of the collective operators  $J_l$  defined in (4) [35]. We will get the same result, however, we can model larger systems this way. For  $\lambda \rightarrow \infty$ , the ground state is the fully polarized state in the  $x$ -direction. For  $\lambda \rightarrow +0$ , it is the Dicke state (11). For intermediate  $\lambda$  values, the ground state is a state which is polarized in the  $x$ -direction and spin squeezed in the  $z$ -direction. We will now find the best precision that can be achieved with this state if we consider estimating  $\theta$  in the unitary dynamics

$$\varrho_\theta = e^{-iJ_y\theta} \varrho_0 e^{+iJ_y\theta}. \quad (28)$$

Figure 2(a) compares the sensitivity we obtained with the optimum defined by the quantum Fisher information. Our bound is close to the optimum when the state is well polarized. It also coincides with the bound in the  $\lambda \rightarrow 0$  limit, when the ground state is close to a Dicke state.

Our next example is a noisy Dicke state of the form

$$\varrho_{\text{th}}(T) \propto \sum_{m=0}^N e^{-\frac{(m-N/2)^2}{T}} |\mathbb{D}_N^{(m)}\rangle \langle \mathbb{D}_N^{(m)}|, \quad (29)$$

where  $N$  is even and  $|\mathbb{D}_N^{(m)}\rangle$  is defined in (10). From (29), we obtain the Dicke state  $|\mathbb{D}_N^{(N/2)}\rangle$  for  $T = 0$ . For  $T > 0$ , other symmetric Dicke states in the vicinity of the state  $|\mathbb{D}_N^{(N/2)}\rangle$  are also populated. The distribution of Dicke states is Gaussian and (29) can be interpreted as a thermal state. We consider again estimating the parameter  $\theta$  in the

dynamics (28). The results can be seen in figure 2(b). Again, our bound is quite close to ultimate bound defined by the quantum Fisher information.

Next, we verify that the dynamics fulfill the condition (15) for both cases considered in this section. In this way we demonstrate that it was justified to use the formula (21) to obtain the precision. Simple algebra shows that if the states considered in our examples are used for metrology as initial states then

$$\text{Tr}(e^{-iJ_y\phi} \varrho e^{+iJ_y\phi} J_z^m) = \text{Tr}(e^{+iJ_y\phi} \varrho e^{-iJ_y\phi} J_z^m) \quad (30)$$

holds for  $m = 2, 4$ , from which (15) follows.

Finally, note that in figure 2(a) and figure 2(b) a metrologically useful  $(k + 1)$ -particle entanglement is detected based on (9) if the quantum Fisher information divided by  $N$  is larger than an integer  $k \ddagger$ . Based on (9), a similar statement holds for  $(\Delta\theta)_{\text{opt}}^{-2}/N$ , which detects entanglement that is useful for the metrological procedure with a  $\langle J_z^2 \rangle$  measurement.

## 5. Applications of the method to experimental data

In this section, we discuss how to apply the formula (21) in the cold gas experiment described in [53]. In the experiment, it is possible to measure the operator  $J_z$ , which is defined as a population difference as

$$J_z = \frac{1}{2}(N_{+1/2} - N_{-1/2}), \quad (31)$$

where  $N_{+1/2}$  and  $N_{-1/2}$  are the number of particles in the spin-states  $j_z = +1/2$  and  $j_z = -1/2$ , respectively. Hence, in principle the expectation values of all moments of  $J_z$  can be obtained. In practice, it is possible to measure the lower order moments like  $\langle J_z^2 \rangle$  and  $\langle J_z^4 \rangle$ , while higher order moments necessitate an increasing number of repetitions of the experiment to get sufficient statistics.

The angular momentum components  $J_x$  and  $J_y$  are measured by rotating the total spin using a  $\frac{\pi}{2}$  microwave coupling pulse before the population difference measurement. Whether  $J_x$  or  $J_y$  is measured depends on the relation between the microwave phase and the phase of the initial Bose-Einstein condensate. The condensate phase represents the only possible phase reference in analogy to the local oscillator in optics. Intrinsically, it has no relation to the microwave phase, such that we homogeneously average over all possible phase relations in our measurements. From another point of view, one can also say that the fluctuation of the phase results in a random rotation of the spin around the  $z$  axis. Hence, we measure

$$J_\alpha = \sin(\alpha)J_x + \cos(\alpha)J_y, \quad (32)$$

where  $\alpha$  is a random phase, and we need to consider an averaging over  $\alpha$ . Effectively, the density matrix of the state is

$$\varrho = \frac{1}{2\pi} \int e^{-iJ_z\phi} \varrho_0 e^{+iJ_z\phi} d\phi, \quad (33)$$

$\ddagger$  This is true if  $k$  is a divisor of  $N$ , or  $k \ll N$  [13, 14].

where  $\varrho_0$  is what we would obtain if we had access to the phase reference  $\S$ . For a state of the form (33), the equality (30) holds for  $m = 2, 4$ , which can be seen directly by substituting (33) into (30). Hence, the unitary dynamics will fulfill the simplifying assumption (15). Note that integration over the rotation angle in (33) does not create quantum entanglement. If the state  $\varrho$  is entangled,  $\varrho_0$  must also be entangled.

Next, we will simplify the bound for the precision of the parameter estimation (21), based on the consequences of our state having the form (33). Since  $\varrho$  is invariant under rotations around the  $z$  axis, we have

$$\langle J_\alpha^m \rangle = \langle J_x^m \rangle = \langle J_y^m \rangle, \quad (34)$$

for all  $m$ . Hence, the expectation values  $\langle J_x^m \rangle$  and  $\langle J_y^m \rangle$  can be obtained from measurements of  $\langle J_\alpha^m \rangle$ . Moreover, there is a single remaining term in (21), the expectation value  $\langle J_z J_x^2 J_z \rangle$ , which is difficult to measure directly in an experiment. It can be bounded as

$$\begin{aligned} \langle J_z J_x^2 J_z \rangle &= \frac{\langle J_z (J_x^2 + J_y^2) J_z \rangle}{2} = \frac{\langle J_z (J_x^2 + J_y^2 + J_z^2) J_z \rangle - \langle J_z^4 \rangle}{2} \\ &\leq \frac{N(N+2)}{8} \langle J_z^2 \rangle - \frac{1}{2} \langle J_z^4 \rangle =: \mathcal{Z}, \end{aligned} \quad (35)$$

where the last inequality is due to (23), which is saturated for symmetric states. Thus, for symmetric states the formula (35) is not only an upper bound, it is exact. Using (34) and (35), we can simplify (21) as

$$(\Delta\theta)_{\text{opt}}^2 \leq \frac{2\sqrt{(\Delta J_z^2)^2 (\Delta J_x^2)^2} + \langle J_x^2 \rangle - 2\langle J_z^2 \rangle (1 + \langle J_x^2 \rangle) + 6\mathcal{Z}}{4(\langle J_x^2 \rangle - \langle J_z^2 \rangle)^2}, \quad (36)$$

where  $\mathcal{Z}$  is defined in (35).

Next, we will substitute the experimentally measured values to (36). The measured data from [49] for  $N = 7900$  yields

$$\begin{aligned} \langle J_z^2 \rangle &= 112 \pm 31, & \langle J_z^4 \rangle &= 40 \times 10^3 \pm 22 \times 10^3, \\ \langle J_x^2 \rangle &= 6 \times 10^6 \pm 0.6 \times 10^6, & \langle J_x^4 \rangle &= 6.2 \times 10^{13} \pm 0.8 \times 10^{13}. \end{aligned} \quad (37)$$

Hence, we obtain for the precision

$$\frac{(\Delta\theta)_{\text{opt}}^{-2}}{N} \geq 3.7 \pm 1.5. \quad (38)$$

In (37) and (38), the statistical uncertainties have been obtained through boot strapping. Note that a direct substitution of the mean values into (36) would yield a gain of 3.3. Based on (6), (38) proves the presence of metrologically useful entanglement [12]. Based on (8), it even indicates that the quantum state had metrologically useful 4-particle entanglement. Within one standard deviation, it demonstrates 3-particle entanglement.

In figure 3, we plot the precision as a function of the rotation angle using the expectation values (37) obtained experimentally. Since we cannot obtain the expectation

$\S$  States of the form (33) can be written as incoherent mixtures of states with a definite  $J_z$ , i.e.,  $\varrho = \sum_{l=-N/2}^{N/2} p_l \varrho_l$ , where for the subensembles  $\langle J_z \rangle_{\varrho_l} = l$  and  $(\Delta J_z)_{\varrho_l}^2 = 0$  hold, while for the probabilities  $p_l \geq 0$  and  $\sum_l p_l = 1$ .

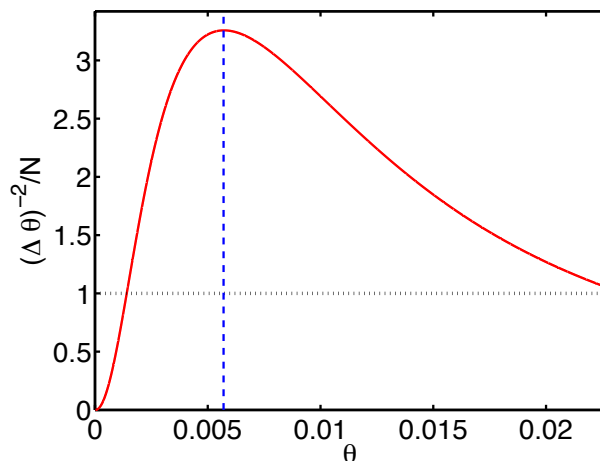


**Figure 3.** (solid)  $(\Delta\theta)^{-2}/N$  as a function of the parameter  $\theta$  given by (18), for parameter values given in (37). (dashed) The maximum is taken at  $\theta = 0.0057$ , as calculated based on (20). (dotted)  $(\Delta\theta)^{-2}/N$  corresponding to the shot-noise limit. If the curve is above this line, then the quantum state shows entanglement based on (6).

value  $\langle J_z J_x^2 J_z \rangle$  experimentally, we approximate it with the right-hand side of (35), i.e., we plot the right-hand side of (36). With that, we overestimate  $(\Delta\theta)^2$ , or equivalently we underestimate  $(\Delta\theta)^{-2}$ .

Thus, we could detect metrological usefulness by measuring the second and fourth moments of the collective angular momentum components. For future applications of our scheme, it is important to further reduce the number of quantities we need to measure for our method. In practice, one can easily avoid the need for determining  $\langle J_x^4 \rangle$ . Note that the distribution of values obtained from measuring  $J_x$  is strongly non-Gaussian. The values  $\pm N/2$  appear most frequently, and the value 0 appear least frequently [47]. One can bound the fourth moment of  $J_x$  as follows

$$\langle J_x^4 \rangle \leq \frac{N^2}{4} \langle J_x^2 \rangle. \quad (39)$$

Equation (39) is based on the fact that for two commuting positive-semidefinite observables,  $A$  and  $B$ , we have

$$\langle AB \rangle \leq \lambda_{\max}(A) \langle B \rangle, \quad (40)$$

where  $\lambda_{\max}(A)$  is the largest eigenvalue of  $A$ . Since even for a noisy Dicke state  $\langle J_x^2 \rangle$  is very large, (39) is a very good upper bound. Substituting the right-hand side of (39) in the place of  $\langle J_x^4 \rangle$  into (36), we will underestimate  $(\Delta\theta)^{-2}$ .

It is also possible to approximate  $\langle J_z^4 \rangle$  with  $\langle J_z^2 \rangle$ . This will not lead to a strict bound on the precision as the one for  $\langle J_x^2 \rangle$ , but still can help us to access the metrological usefulness based on second moments only. One can use the formula

$$\langle J_z^4 \rangle = \beta \langle J_z^2 \rangle^2, \quad (41)$$

where  $\beta$  is a constant. In principle,  $\beta$  can be obtained based on some knowledge of the distribution of the measured values. In practice, the distribution is typically dominated

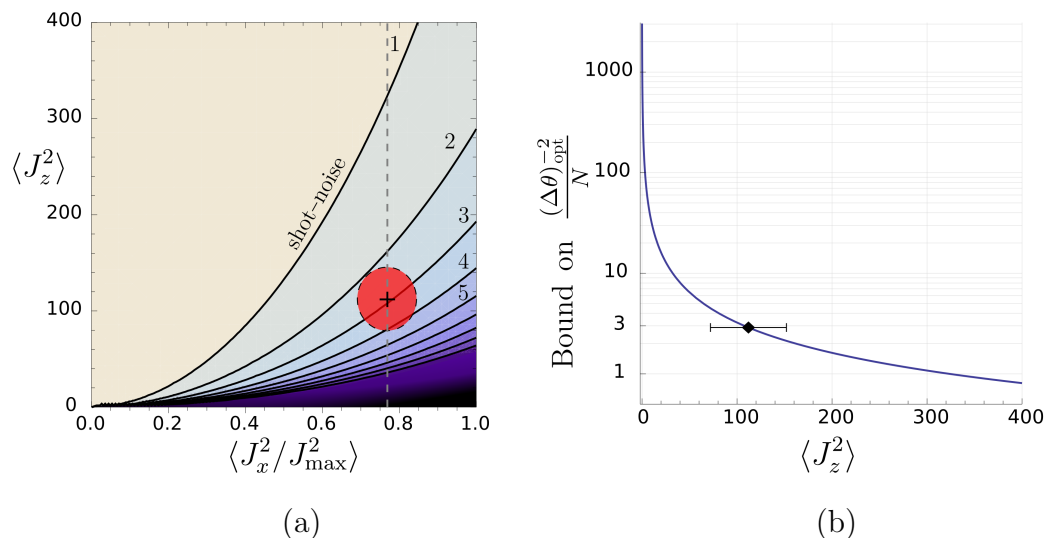


**Figure 4.** (a) Lower bound on  $(\Delta\theta)^{-2}$  as a function of  $\langle J_x^2 \rangle$  and  $\langle J_z^2 \rangle$  for an ensemble of  $N = 7900$  particles. For all points in a region with index  $k$ , the precision is bounded according to  $(\Delta\theta)^{-2} > (k - 1)N$ , and the state possesses at least  $k$ -particle entanglement [see (9)]. Any state corresponding to points below the curve labelled "shot-noise" is entangled. The lower bound on  $(\Delta\theta)^{-2}$  is based on (36). In addition, (39) is used to bound  $\langle J_x^4 \rangle$  and a Gaussian distribution is assumed for the measurement results of  $J_z$ . Note that the horizontal axis is normalized by  $J_{\max}^2$  which equals  $\langle J_x^2 \rangle$  for Dicke states given in (24). The cross and the uncertainty ellipse correspond to the experimental results given in (37). (b) A cross section corresponding to the vertical dashed line in figure (a). The uncertainty for the error bar is taken from (37).

by a Gaussian technical noise. For a Gaussian distribution and for large  $N$ , we have  $\beta = 3$ . Note that the distribution is expected to be centered around zero, since the method used to create a Dicke state makes sure that  $\langle J_z \rangle = 0$  [47, 49]. Thus, (41) can give an estimate on the fourth moment, even if only the second moments are measured, under the assumption of a Gaussian probability density.

Substituting (39) and (41) into (36), we obtain a formula that gives an upper bound on  $(\Delta\theta)^2$  merely as a function of  $\langle J_x^2 \rangle$ ,  $\langle J_z^2 \rangle$  and  $\beta$ . It is reasonable to choose  $\beta = 3$  assuming a Gaussian statistics for the measurement results of  $J_z$ . Figure 4(a) shows the two-dimensional plot which is obtained based on these considerations. The regions with various levels of multipartite entanglement can clearly be identified. The ideal Dicke state (11) corresponds to the bottom-right corner. In figure 4(b), the cross section of the two-dimensional plot is shown. Note that calculations based only on the second moments give a metrological usefulness different from (38), which used information also on the fourth order moments. Finally, also note that a figure similar to figure 4(a) appears in [53], where multipartite entanglement has been detected independently from metrology.

## 6. Conclusions

We have discussed how to access the metrological usefulness of noisy Dicke states for estimating the angle of rotation. Our formula is able to verify the metrological usefulness without carrying out the metrological task. We have demonstrated the use of our formula for recent experimental results. The metrological usefulness can be inferred from measurements of second and the fourth moments of the  $x$ -component and the  $z$ -component of the collective angular momentum only. In practice, the fourth-order moments can be well approximated by the second-order moments. After completing our calculations, we have recently become aware of a related work by Haine *et al.* [69], which is based on the preliminary work in [70], and obtains sensitivity bounds for metrology with twin-Fock states.

## Acknowledgments

We thank S. Altenburg, R. Demkowicz-Dobrzański, F. Fröwis, O. Gühne, P. Hyllus, M. Kleinmann, M. W. Mitchell, M. Modugno, L. Pezze, L. Santos, A. Smerzi, I. Urizar-Lanz, and G. Vitagliano for stimulating discussions. We are thankful for the support of the EU (ERC Starting Grant 258647/GEDENTQOPT, CHIST-ERA QUASAR, the MINECO (Project No. FIS2012-36673-C03-03), the Basque Government (Project No. IT4720-10), UPV/EHU Program No. UFI 11/55, the OTKA (Contract No. K83858). We acknowledge support from the Centre QUEST, the DFG (Research Training Group 1729), and the EMRP, which is jointly funded by the EMRP participating countries within EURAMET and the European Union.

## Appendix A. Details of the derivation of (16) and (17) using the symmetry (15)

In this appendix, we discuss how we use the symmetry (15) to simplify our calculations.

First, let us see the numerator of (13). Based on (14), the dynamics of the second and the fourth moments are obtained, respectively, as

$$\begin{aligned}
 \langle J_z^2(\theta) \rangle &= \langle J_z^2 \rangle \cos^2 \theta + \langle J_x^2 \rangle \sin^2 \theta - \langle \{J_z, J_x\} \rangle \sin \theta \cos \theta, \\
 \langle J_z^4(\theta) \rangle &= \langle J_z^4 \rangle \cos^4 \theta + \langle J_x^4 \rangle \sin^4 \theta \\
 &\quad + \left( \langle \{J_z, J_x\}^2 \rangle + \langle \{J_z^2, J_x^2\} \rangle \right) \cos^2 \theta \sin^2 \theta \\
 &\quad - \langle A \rangle \cos \theta \sin^3 \theta - \langle B \rangle \cos^3 \theta \sin \theta.
 \end{aligned} \tag{A.1}$$

where  $A = \{J_z^2, J_x J_z + J_z J_x\}$ , and  $B = \{J_x^2, J_x J_z + J_z J_x\}$ . After calculating the terms in the numerator of (13), for the derivative in the denominator of (13) we obtain

$$\partial_\theta \langle J_z^2 \rangle = 2(\langle J_x^2 \rangle - \langle J_z^2 \rangle) \cos \theta \sin \theta + \langle \{J_z, J_x\} \rangle (\cos^2 \theta - \sin^2 \theta). \tag{A.2}$$

For calculating (A.2), we used the dynamics of  $\langle J_z^2(\theta) \rangle$  given in (A.1).

Let us use now the assumption (15) to simplify the equations (A.1) and (A.2). From (15) it follows that the coefficients of all terms that are odd functions of  $\theta$  must be zero. First, let us consider the equation giving the dynamics of  $\langle J_z^2(\theta) \rangle$  in (A.1). We realize that

$$\langle \{J_z, J_x\} \rangle = 0 \quad (\text{A.3})$$

must hold. Then, we set the coefficients of all other terms that are odd functions of  $\theta$  to zero. Hence, from (A.1) we arrive at (16). In a similar way, using (A.3), from (A.2) we arrive at (17).

Finally, as we discussed before, the experimentally prepared state has the symmetry (15), which is also an assumption used to derive (21). Let us examine the case of an initial state  $\varrho$  that does not have this property. Let us define now the state

$$\varrho_z = \sigma_z^{\otimes N} \varrho \sigma_z^{\otimes N}, \quad (\text{A.4})$$

Direct substitution of (A.4) into (A.1) shows that

$$\begin{aligned} \langle J_z^2(\theta) \rangle_{\varrho} &= \langle J_z^2(-\theta) \rangle_{\varrho_z}, \\ \langle J_z^4(\theta) \rangle_{\varrho} &= \langle J_z^4(-\theta) \rangle_{\varrho_z}. \end{aligned} \quad (\text{A.5})$$

Hence, the state

$$\varrho_s = \frac{1}{2}(\varrho + \sigma_z^{\otimes N} \varrho \sigma_z^{\otimes N}), \quad (\text{A.6})$$

obeys the symmetry (15). Note that the transformation (A.6) does not change the quantities in (18) and in (21). Thus, in a sense with our scheme we get information on the metrological usefulness of the state  $\varrho_s$ , that we would get after the trivial mixing operation (A.6).

## Appendix B. Details of the calculations for (18)

In this appendix, we give further details of our calculations for obtaining (18). After straightforward but long algebra based on commutation relations, the coefficient of the term  $\cos^2 \theta \sin^2 \theta$  in (16) can be obtained as

$$\langle \{J_z, J_x\}^2 \rangle + \langle \{J_z^2, J_x^2\} \rangle = 4\langle J_x^2 \rangle - 3\langle J_y^2 \rangle - 2\langle J_z^2 \rangle + 6\langle J_z J_x^2 J_z \rangle. \quad (\text{B.1})$$

Then, based on (13), (16), (17), and (B.1), we can write the variance of the estimated parameter  $\theta$  in the following way

$$(\Delta\theta)^2 = \frac{(\Delta J_z^2)^2 \cos^4 \theta + (\Delta J_x^2)^2 \sin^4 \theta + \mathcal{C} \cos^2 \theta \sin^2 \theta}{4(\langle J_x^2 \rangle - \langle J_z^2 \rangle)^2 \cos^2 \theta \sin^2 \theta}, \quad (\text{B.2})$$

where

$$\mathcal{C} := 4\langle J_x^2 \rangle - 3\langle J_y^2 \rangle - 2\langle J_z^2 \rangle + 6\langle J_z J_x^2 J_z \rangle - 2\langle J_x^2 \rangle \langle J_z^2 \rangle. \quad (\text{B.3})$$

Simplifying and rearranging terms in (B.2), we arrive at (18). Note that without the assumption (15), we could not have obtained a formula with so simple dependence on  $\theta$ .

- [1] Giovannetti V, Lloyd S and Maccone L 2004 *Science* **306** 1330–1336
- [2] Paris M G A 2009 *Int. J. Quant. Inf.* **07** 125–137
- [3] Demkowicz-Dobrzański R, Jarzyna M and Kołodyński J 2015 *Prog. Opt.* **60** 345 – 435 (*Preprint arXiv:1405.7703*)
- [4] Pezze L and Smerzi A 2014 Quantum theory of phase estimation *Atom Interferometry (Proc. Int. School of Physics 'Enrico Fermi', Course 188, Varenna)* ed Tino G and Kasevich M (IOS Press, Amsterdam) pp 691–741 (*Preprint arXiv:1411.5164*)
- [5] Schaff J F, Langen T and Schmiedmayer J 2014 Interferometry with atoms *Atom Interferometry (Proc. Int. School of Physics 'Enrico Fermi', Course 188, Varenna)* ed Tino G and Kasevich M (IOS Press, Amsterdam) pp 1–87 (*Preprint arXiv:1504.04285*)
- [6] Helstrom C 1976 *Quantum Detection and Estimation Theory* (Academic Press, New York)
- [7] Holevo A 1982 *Probabilistic and Statistical Aspects of Quantum Theory* (North-Holland, Amsterdam)
- [8] Braunstein S L and Caves C M 1994 *Phys. Rev. Lett.* **72** 3439–3443
- [9] Braunstein S L, Caves C M and Milburn G J 1996 *Ann. Phys.* **247** 135–173
- [10] Petz D 2008 *Quantum information theory and quantum statistics* (Springer, Berlin, Heilderberg)
- [11] Tóth G and Apellaniz I 2014 *J. Phys. A: Math. Theor.* **47** 424006
- [12] Pezzé L and Smerzi A 2009 *Phys. Rev. Lett.* **102** 100401
- [13] Hyllus P, Laskowski W, Krischek R, Schwemmer C, Wiecezorek W, Weinfurter H, Pezzé L and Smerzi A 2012 *Phys. Rev. A* **85** 022321
- [14] Tóth G 2012 *Phys. Rev. A* **85** 022322
- [15] Hyllus P, Gühne O and Smerzi A 2010 *Phys. Rev. A* **82** 012337
- [16] Escher B, de Matos Filho R and Davidovich L 2011 *Nat. Phys.* **7** 406–411
- [17] Demkowicz-Dobrzański R, Kołodyński J and Guță M 2012 *Nat. Commun.* **3** 1063
- [18] Leibfried D, Barrett M, Schaetz T, Britton J, Chiaverini J, Itano W, Jost J, Langer C and Wineland D 2004 *Science* **304** 1476–1478
- [19] Napolitano M, Koschorreck M, Dubost B, Behbood N, Sewell R J and Mitchell M W W 2011 *Nature* **471** 486–489
- [20] Riedel M F, Böhi P, Li Y, Hänsch T W, Sinatra A and Treutlein P 2010 *Nature* **464** 1170–1173
- [21] Gross C, Zibold T, Nicklas E, Estève J and Oberthaler M K 2010 *Nature* **464** 1165–1169
- [22] Demkowicz-Dobrzański R, Banaszek K and Schnabel R 2013 *Phys. Rev. A* **88** 041802
- [23] Gross C 2012 *J. Phys. B: At. Mol. Opt. Phys.* **45** 103001
- [24] Hald J, Sørensen J L, Schori C and Polzik E S 1999 *Phys. Rev. Lett.* **83** 1319–1322
- [25] Fernholz T, Krauter H, Jensen K, Sherson J F, Sørensen A S and Polzik E S 2008 *Phys. Rev. Lett.* **101** 073601
- [26] Wasilewski W, Jensen K, Krauter H, Renema J J, Balabas M V and Polzik E S 2010 *Phys. Rev. Lett.* **104** 133601
- [27] Sewell R J, Koschorreck M, Napolitano M, Dubost B, Behbood N and Mitchell M W 2012 *Phys. Rev. Lett.* **109**(25) 253605
- [28] Appel J, Windpassinger P J, Oblak D, Hoff U B, Kaergaard N and Polzik E S 2009 *Proc. Natl. Acad. Sci. U.S.A.* **106** 10960–10965
- [29] Hammerer K, Sørensen A S and Polzik E S 2010 *Rev. Mod. Phys.* **82** 1041–1093
- [30] Estève J, Gross C, Weller A, Giovanazzi S and Oberthaler M 2008 *Nature* **455** 1216–1219
- [31] Ockeloen C F, Schmied R, Riedel M F and Treutlein P 2013 *Phys. Rev. Lett.* **111**(14) 143001
- [32] Muessel W, Strobel H, Linnemann D, Hume D B and Oberthaler M K 2014 *Phys. Rev. Lett.* **113** 103004
- [33] Kitagawa M and Ueda M 1993 *Phys. Rev. A* **47** 5138–5143
- [34] Wineland D J, Bollinger J J, Itano W M and Heinzen D J 1994 *Phys. Rev. A* **50** 67–88
- [35] Sørensen A S and Mølmer K 2001 *Phys. Rev. Lett.* **86** 4431–4434
- [36] Ma J, Wang X, Sun C P and Nori F 2011 *Phys. Rep.* **509** 89–165
- [37] Greenberger D M, Horne M A, Shimony A and Zeilinger A 1990 *Am. J. Phys.* **58** 1131



- [38] Bouwmeester D, Pan J W, Daniell M, Weinfurter H and Zeilinger A 1999 *Phys. Rev. Lett.* **82** 1345
- [39] Pan J W, Bouwmeester D, Daniell M, Weinfurter H and Zeilinger A 2000 *Nature* **403** 515
- [40] Zhao Z, Yang T, Chen Y A, Zhang A N, Żukowski M and Pan J W 2003 *Phys. Rev. Lett.* **91** 180401
- [41] Lu C Y, Zhou X Q, Gühne O, Gao W B, Zhang J, Yuan Z S, Goebel A, Yang T and Pan J W 2007 *Nat. Phys.* **3** 91–95
- [42] Gao W B, Lu C Y, Yao X C, Xu P, Gühne O, Goebel A, Chen Y A, Peng C Z, Chen Z B and Pan J W 2010 *Nat. Phys.* **6** 331–335
- [43] Sackett C, Kielpinski D, King B, Langer C, Meyer V, Myatt C, Rowe M, Turchette Q, Itano W, Wineland D and Monroe C 2000 *Nature* **404** 256–259
- [44] Monz T, Schindler P, Barreiro J T, Chwalla M, Nigg D, Coish W A, Harlander M, Hänsel W, Hennrich M and Blatt R 2011 *Phys. Rev. Lett.* **106** 130506
- [45] Urizar-Lanz I, Hyllus P, Egusquiza I L, Mitchell M W and Tóth G 2013 *Phys. Rev. A* **88** 013626
- [46] Behbood N, Martin Ciurana F, Colangelo G, Napolitano M, Tóth G, Sewell R J and Mitchell M W 2014 *Phys. Rev. Lett.* **113** 093601
- [47] Lücke B, Scherer M, Kruse J, Pezzé L, Deuretzbacher F, Hyllus P, Peise J, Ertmer W, Arlt J, Santos L, Smerzi A and Klempt C 2011 *Science* **334** 773–776
- [48] Hamley C, Gerving C, Hoang T, Bookjans E and Chapman M 2012 *Nat. Phys.* **8** 305–308
- [49] Krischek R, Schwemmer C, Wiecek W, Weinfurter H, Hyllus P, Pezzé L and Smerzi A 2011 *Phys. Rev. Lett.* **107** 080504
- [50] Prevedel R, Cronenberg G, Tame M S, Paternostro M, Walther P, Kim M S and Zeilinger A 2009 *Phys. Rev. Lett.* **103** 020503
- [51] Zhang Z and Duan L M 2014 *New J. Phys.* **16** 103037
- [52] Fröwis F and Gisin N 2014 *arXiv:1409.4440*
- [53] Lücke B, Peise J, Vitagliano G, Arlt J, Santos L, Tóth G and Klempt C 2014 *Phys. Rev. Lett.* **112** 155304
- [54] Werner R F 1989 *Phys. Rev. A* **40** 4277–4281
- [55] Horodecki R, Horodecki P, Horodecki M and Horodecki K 2009 *Rev. Mod. Phys.* **81** 865–942
- [56] Acín A, Bruß D, Lewenstein M and Sanpera A 2001 *Phys. Rev. Lett.* **87** 040401
- [57] Gühne O, Tóth G and Briegel H J 2005 *New J. Phys.* **7** 229
- [58] Dicke R H 1954 *Phys. Rev.* **93** 99–110
- [59] Eibl M, Kiesel N, Bourennane M, Kurtsiefer C and Weinfurter H 2004 *Phys. Rev. Lett.* **92** 077901
- [60] Häffner H, Hänsel W, Roos C, Benhelm J, Chwalla M, Körber T, Rapol U, Riebe M, Schmidt P, Becher C, Gühne O, Dür W and Blatt R 2005 *Nature* **438** 643–646
- [61] Haas F, Volz J, Gehr R, Reichel J and Esteve J 2014 *Science* **344** 180–183
- [62] Tóth G 2007 *J. Opt. Soc. Am. B* **24** 275–282
- [63] Tóth G, Wiecek W, Krischek R, Kiesel N, Michelberger P and Weinfurter H 2009 *New J. Phys.* **11** 083002
- [64] Holland M J and Burnett K 1993 *Phys. Rev. Lett.* **71** 1355–1358
- [65] Kiesel N, Schmid C, Tóth G, Solano E and Weinfurter H 2007 *Phys. Rev. Lett.* **98** 063604
- [66] Wiecek W, Krischek R, Kiesel N, Michelberger P, Tóth G and Weinfurter H 2009 *Phys. Rev. Lett.* **103** 020504
- [67] Chiuri A, Greganti C, Paternostro M, Vallone G and Mataloni P 2012 *Phys. Rev. Lett.* **109** 173604
- [68] Schindler P, Müller M, Nigg D, Barreiro J T, Martinez E, Hennrich M, Monz T, Diehl S, Zoller P and Blatt R 2013 *Nat. Phys.* **9** 361–367
- [69] Haine S A, Szigeti S S, Lang M D and Caves C M 2015 *Phys. Rev. A* **91** 041802
- [70] Szigeti S S, Tonekaboni B, Lau W Y S, Hood S N and Haine S A 2014 *Phys. Rev. A* **90** 063630